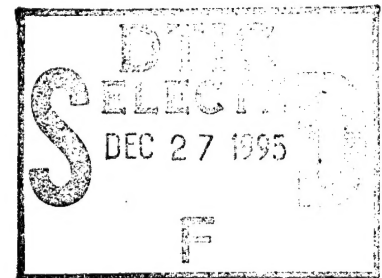PL-TR-95-2104

IDENTIFICATION OF PRESUMED SHALLOW UNDERWATER CHEMICAL BLASTS USING LAND-BASED REGIONAL ARRAYS

Douglas Baumgardt

ENSCO, Inc.
Signal Analysis and Systems Division
5400 Port Royal Road
Springfield, Virginia   22151-2312

DTIC
ELECTE
DEC 27 1995
F

24 July 1995

Scientific Report No. 2

PHILLIPS LABORATORY
Directorate of Geophysics
AIR FORCE MATERIEL COMMAND
HANSCOM AFB, MA   01731-3010

19951219 020

DTIC QUALITY INSPECTED 1

REPORT DOCUMENTATION PAGE

Form Approved
OMB No. 0704-0188

1. AGENCY USE ONLY (Leave blank)	2. REPORT DATE	3. REPORT TYPE AND DATES COVERED
	24 July 1995	Scientific Report #2

4. TITLE AND SUBTITLE
Identification of Presumed Shallow Underwater Chemical Blasts Using Land-Based Regional Arrays

5. FUNDING NUMBERS
PE 62301E
PR NM 93 TA GM WU AC
Contract F19628-93-C-0103

6. AUTHOR(S)

Douglas R. Baumgardt

7. PERFORMING ORGANIZATION NAME(S) AND ADDRESS(ES)

ENSCO, Inc.
Signal Analysis and Systems Division
5400 Port Royal Road
Springfield, Virginia 22151-2312

8. PERFORMING ORGANIZATION REPORT NUMBER

SAS-TR-95-118

9. SPONSORING/MONITORING AGENCY NAME(S) AND ADDRESS(ES)

Phillips Laboratory
29 Randolph Road
Hanscom AFB, Massachusetts 01731-3010

Contract Manager: James Lewkowicz/GPE

10. SPONSORING/MONITORING AGENCY REPORT NUMBER

PL-TR-95-2104

11. SUPPLEMENTARY NOTES

12a. DISTRIBUTION/AVAILABILITY STATEMENT

Approved for public release; distribution unlimited

12b. DISTRIBUTION CODE

13. ABSTRACT (Maximum 200 words)
Seismic events located in the Gulf of Bothnia and in the Baltic Sea, recorded at the regional seismic arrays NORESS and FINESA, have characteristics of underwater blasts observed hydroacoustically. Spectral analysis of regional phases associated with the events reveals strong time-independent spectral scalloping indicating that the waveforms are made up of pulse-echo pairs. Cepstral analysis gives consistent delays times between the pulse-echo pairs with the most common delays between 400 and 600 ms. Some cepstra have peaks at quefrencies of 150 to 350 ms. The cepstral peaks are observed in all phases associated with the event, recorded at NORESS and FINESA, and events recorded at both arrays have the same delay times. The higher time delays appear to be consistent with bubble pulse delays commonly observed in underwater blasts recorded hydroacoustically. The lower quefrency peaks appear to be negative perhaps caused by echoes with reversed polarities relative to the primary pulse and are consistent with being water column reverberations. Multiple frequency analysis of the *Pn/Lg* amplitude ratios shows that the Baltic Sea events have high ratios comparable to nearby mine blasts on land and clearly discriminate from earthquakes in the region. However, the Gulf of Bothnia events have *Pn/Lg* ratios less than one across the entire frequency band up to 8 to 10 Hz which more closely resemble earthquakes that blasts. Yet, these events have strong spectral modulations not observed in earthquakes which strongly suggests that they were underwater blasts. The strong shear waves from the underwater blasts may result from scattering in the sea bottom sediments. This study shows the efficacy of seismic sensors to monitor offshore environments for possible clandestine nuclear explosion tests. The regional *Pn/Lg* ratio discriminant alone cannot always be relied upon to identify blasting activity and broadband analysis of bubble pulse spectral modulations must also be done. Evasion scenarios where underwater blasts can be detonated with no bubble pulse (e.g., very shallow blasts) and have large shear waves may need to be considered.

14. SUBJECT TERMS
Discrimination, Seismology, Underwater Blasts, Bubble Pulse, Comprehensive Test Ban Treaty

15. NUMBER OF PAGES
38

16. PRICE CODE

17. SECURITY CLASSIFICATION OF REPORT	18. SECURITY CLASSIFICATION OF THIS PAGE	19. SECURITY CLASSIFICATION OF ABSTRACT	20. LIMITATION OF ABSTRACT
Unclassified	Unclassified	Unclassified	SAR

TABLE OF CONTENTS

INTRODUCTION

The problem of the identification of underwater blasts has gained increased interest recently in the context of the monitoring of a possible comprehensive test ban treaty (CTBT). At the recent CTBT Monitoring Technologies Conference, held in Sand Diego in September of 1994, a number of papers were presented which reviewed how the hydro-acoustic method can be used to monitor underwater explosions. Underwater explosions can be identified by distinctive features, primarily bubble-pulse signatures and fast rise times, recorded on high frequency hydroacoustic signals. These signatures may be observable over distance ranges in the ocean in excess of 1000 km because of the unique propagation conditions in the SOFAR channel of the deep ocean. Some of the papers at the CTBT Conference (e.g., Phillips, 1994) suggested that these kinds of signatures could only uniquely be detected and analyzed using hydoacoustic sensors, and that seismic sensors had limited utility because of their location and limited bandwidth.

The purpose of this paper is to point out that land-based seismic sensors can and have been used to detect and identify underwater explosions, and that hydroacoustic sensors are not always required. Presumed underwater explosions have been detected by the regional array system in Scandinavia (NORESS, FINESA, ARCESS) and examples of these events will be presented in this paper. Techniques and systems used to discriminate explosions and earthquakes on land can also be used to identify events in the oceans using seismic recordings.

Land-based seismic sensors may serve best for monitoring for explosions near the coast in shallow-water environments, and the examples of presumed underwater blasts presented in this paper fall in this category. Some concern has been expressed that event identification of underwater blasts near the coast may be problematic using long range hydroacoustic sensors because of the shallow water environment, energy-absorbing silt layers at the bottom, and a distorted sound channel may result in poor sound propagation conditions (White et al, 1995). In these situations, land-based sensors within a few hundred kilometers of the coast may be more effective at detecting the seismic signals which couple into the earth than would hydroacoustic sensors in detecting the hydroacoustic signals propagating over a longer distance through the laterally heterogeneous sound channel.

In this paper, we first discuss the seismic data recorded at the regional arrays from presumed blasts in the shallow-water environments of the Gulf of Bothnia and the Baltic Sea. The blasts are called "presumed underwater blasts" because, although seismic sensors

1

located the events offshore, we have no ground truth at present to confirm that they were actually underwater sources. We then discuss the signal analysis techniques from the Intelligent Seismic Event Identification System (ISEIS) (Baumgardt et al, 1991b) that indicates that the events were blasts set off in the shallow marine environment. In addition to showing the utility of narrow-band seismic sensors for monitoring underwater explosions, this paper also demonstrates how synergy between seismic and hydroacoustic methods for identification can be achieved by using seismic signal analysis techniques on both seismic and hydroacoustic data.

EVENT LOCATIONS AND PROPAGATION PATHS

Figure 1(a) shows the locations of the events in the Gulf of Bothnia off the east coast of Sweden and in the Baltic near southern Norway which we believe to be underwater blasts. Tables 1 and 2 list the event parameters, determined by the Intelligent Monitoring System (IMS), along with the assigned event numbers, called the ORIDs.

Table 1 below lists the locations of the events located in the Gulf of Bothnia.

Table 1: Source Parameter for Presumed Explosions and Earthquakes in the Gulf of Bothnia

ORID	DATE	Origin Time	Latitude (Deg. N.)	Longitude (Deg. E)	Local Magnitude	Source Type
70 [1]	09/24/85	09:55:37	60.90	20.40	2.2	Exp [2]
366137	05/05/92	14:05:13	58.89	18.17	1.6	Exp [2]
366138	05/06/92	08:01:11	59.04	18.17	1.6	Exp [2]
366139	05/18/92	13:37:03	58.76	18.16	1.7	Exp [2]
366145	09/09/92	22:34:51	59.00	18.23	2.0	Exp [2]
202414	08/22/90	04:08:30	63.86	20.81	2.1	Eq [3]

(1) This event only recorded at NORESS. Event location from Helsinki bulletin.
(2) Underwater explosion source types are presumed.
(3) Earthquake identification based on felt reports in Scandinavia.

The events labeled Region 1 in Figure 1(a) are events in the Gulf of Bothnia east of Sweden which were recorded at the FINESA and NORESS arrays with ORIDs 366137, 366138, 366139, and 366145. These events were located by the Intelligent Monitoring System (IMS) (Bache et al, 1990). These events occurred in the same region as the
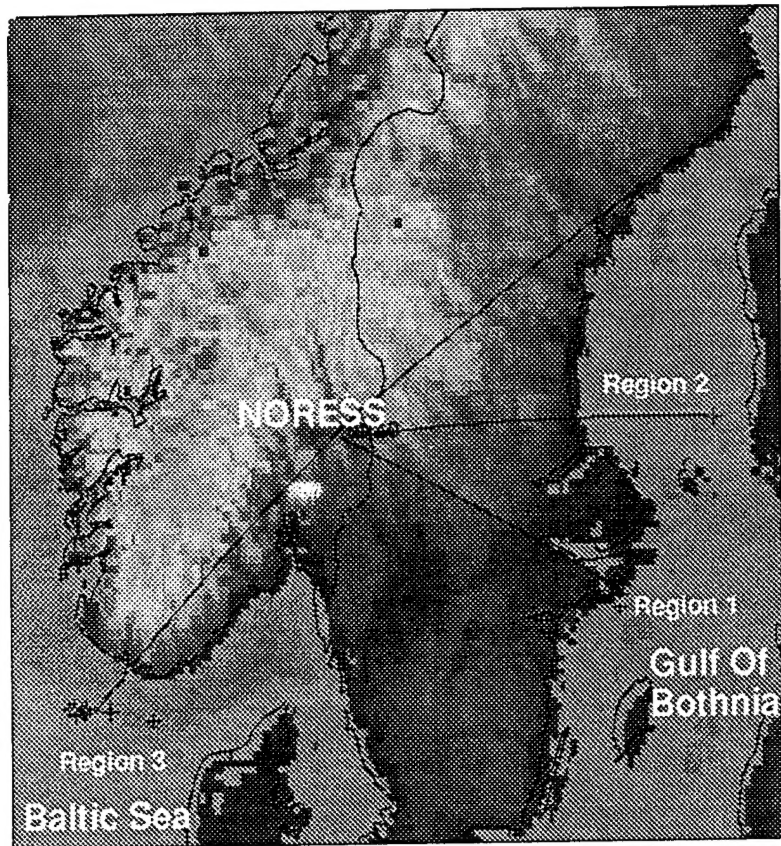
Figure 1: (a) Topographic map showing locations of the presumed underwater explosions and the propagation paths to the NORESS (NRA0) array.

sources for Project BABEL (BABEL Working Group, 1993) although we have no information that these events were associated with this program.

Region 2 contains an event in 1985, with ORID 70 in Table 1, which was listed in the Helsinki seismic bulletin and was recorded only at NORESS. (The FINESA array had not yet been installed.) This event occurred in an aseismic region in the middle of the Gulf of Bothnia, which suggests that the event may actually have been an explosion.

The Region 3 event parameters, shown in Figure 1(a), are given below in Table 2.

Table 2: Source Parameter for Presumed Explosions and an Earthquake in the Offshore Stavenger Region of Southern Norway Recorded at NORESS

ORID	DATE	Origin Time	Latitude (Deg N.)	Longitude (Deg. E)	Local Magnitude	Source Type
58	11/20/85	22:10:44	57.61	5.67	2.3	Exp [1]
59	11/20/85	22:24:38	57.66	5.72	2.2	Exp [1]
60	11/20/85	22:57:11	57.63	6.27	2.2	Exp [1]
61	11/20/85	23:10:47	57.66	5.35	2.3	Exp [1]
62	11/20/85	23:17:29	57.69	5.45	2.3	Exp [1]
63	11/20/85	23:23:10	57.64	5.62	2.2	Exp [1]
64	11/20/85	23:28:23	57.58	5.49	2.2	Exp [1]
192482	02/26/90	20:30:16	57.51	7.27	3.06	Eq [2]

(1) Underwater source types are presumed. Locations from Suteau-Henson and Bache (1988).
(2) Earthquake identification based on felt reports in Norway. Location determined by IMS.

Region 3, which we call the Stavenger offshore region, contains a group of presumed underwater blasts (ORIDs 58 through 64 in Table 2) originally studied by Suteau-Henson and Bache (1988). They called these events earthquakes because of their location in the Baltic Sea. Also included in Region 3 is a felt earthquake (ORID=192482) which will compared with the presumed blasts for discrimination purposes.

Figures 1(b), (c), and (d) show bathymetric cross sections from Regions 1, 2, and 3 to the NORESS array. The horizontal dashed line indicates sea level and the solid line shows the bathymetry in meters. For the events in the Gulf of Bothnia, Regions 1 and 2, the maximum water depths along the path are on the order of 50 to 100 m. The water depths in the Stavenger offshore region in the Baltic Sea, Region 3, are between 175 and 380 m.

4
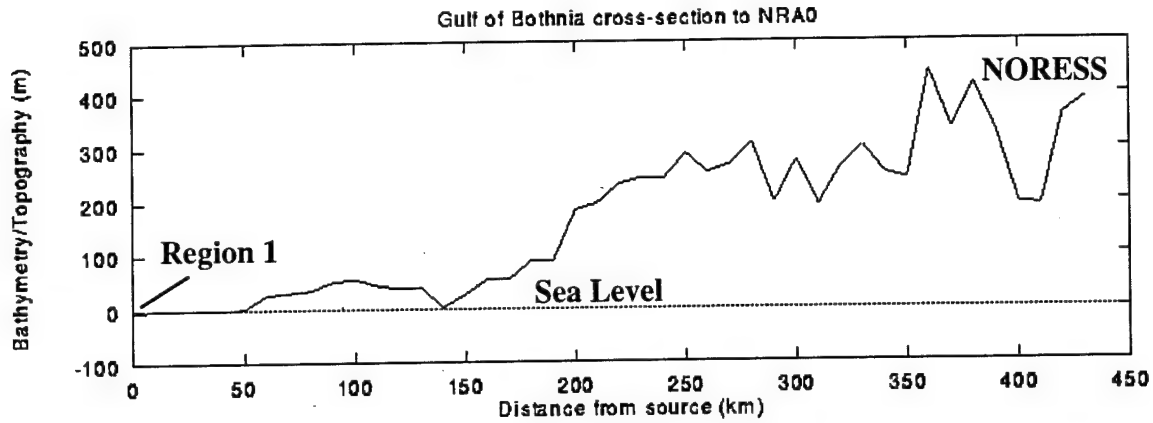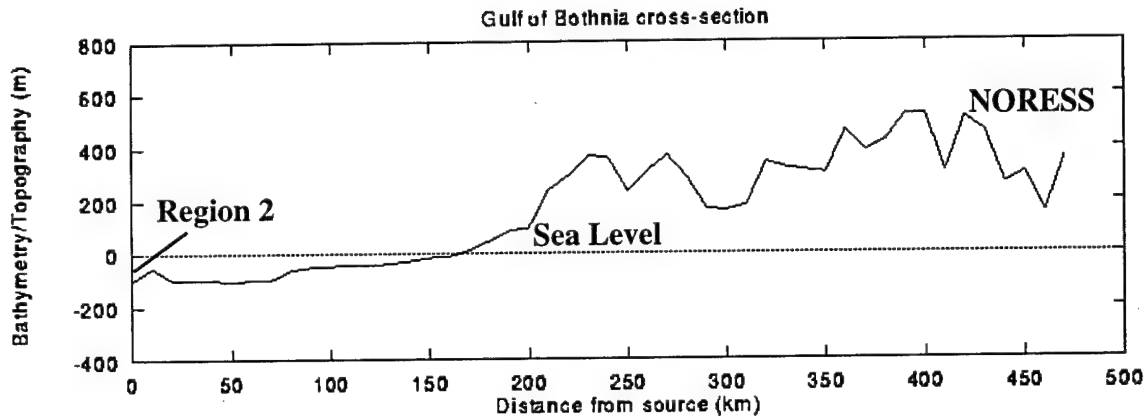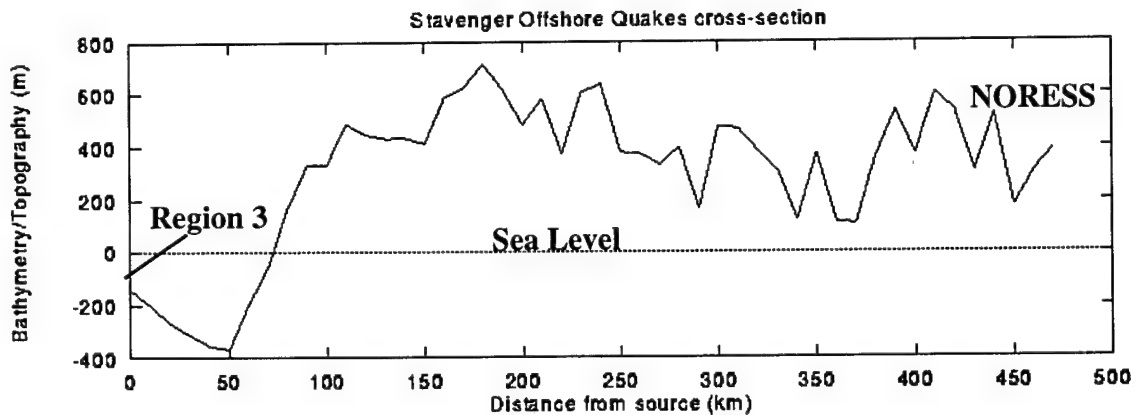
Figure 1: (b,c,d) Bathymetric/topographic cross sections for the propagation paths to the NORESS array (NRA0) from the three underwater explosion regions shown on the map in Figure 2(a). (b) East Coast of Sweden - Gulf of Bothnia (Region 1), (c) Central Gulf of Bothnia (Region 2), (d) Baltic Sea - Stavenger offshore region (Region 3).

5

Figure 2(a) shows the great circle path on a topographic map from Region 1 to FINESA. The bathymetric cross section for this path is shown in Figure 2(b). This path has water depths between 50 to 75 m in the distance range of 100 to 200 km from the source region. As shown in the figure, some of the events are located near the coast and on land. However, the 95% confidence ellipse axes of the IMS locations are between 7 and 14 km for the semiminor axes and 24 to 50 km for the semimajor axes.

Although we have no ground-truth to confirm that these events were underwater explosions, their estimated locations place them well offshore. We show in this paper that the waveform characteristics are definitely consistent with these events being underwater explosions in these near-coastal regions.

SPECTRAL/CEPSTRAL ANALYSIS

One of the most direct ways of detecting underwater explosions is to detect bubble pulses. Hydroacoustic studies (e.g., Mitchell et al, 1976; Urich, 1983) have shown how bubble pulse delay times can be inferred from spectral modulation periods. Baumgardt and Ziegler (1988) showed how time-independent spectral modulations produced by ripple-fired mine blasts could be identified by finding peaks in cepstra derived from the spectra. An automated method for finding time-independent cepstral peaks, called the Multiple Event Recognition System (MERSY), was described by Baumgardt et al (1991a). The same method should work to identify bubble pulses, since they are like ripple fired blasts in that the bubble pulse would be an "echo" of the primary pulse produced by the explosion in the water. Studies of acoustic data have shown that the differences in the peaks and troughs of the spectral modulation may be as great as 6 to 10 dB at distances of hundreds of miles (Mitchell et al, 1976). The primary and first bubble pulse should act as delayed sources with each generating a full complement of regional phases when recorded seismically.

Figure 3(a) shows an example of one of the Region 1 events, ORID = 366137, recorded at one of the array elements (FIB2) in the FINESA array (FIA0). The phase identifications of the analyst are indicated with the lines. The four regional phases identified as Pn, Pg, Sn, and Lg, clearly have high signal-to-noise ratio. Figure 3(b) shows the waveform zoomed over the four second time interval from 159.1 seconds to 162.1 seconds in the Pn wavetrain. This zoomed waveform reveals a pulse-echo type pattern in the waveform which repeats at intervals of about one time interval, which is about 0.5 seconds. We
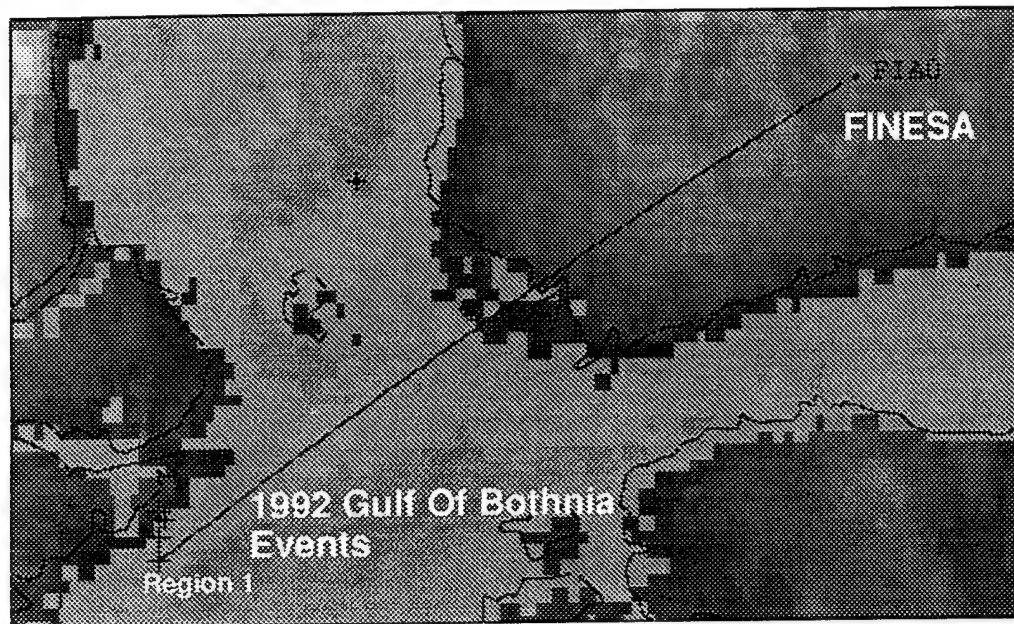
(a)
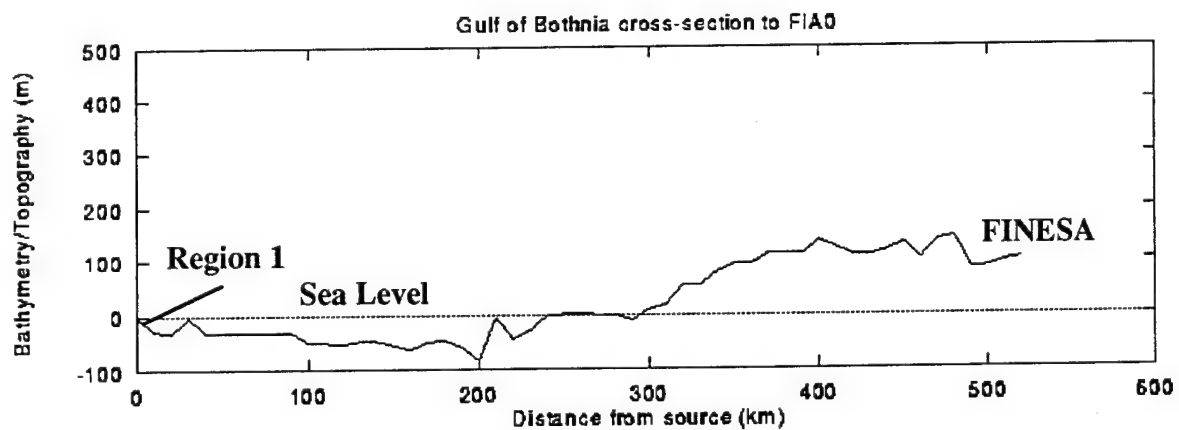
(b)

Figure 2: (a) Topographic map showing the propagation path from the 1992 presumed underwater blasts in Region 1, east coast of Sweden, to the FINESA array (FIA0). (b) Bathymetric/topographic cross section for the propagation path shown in (a).
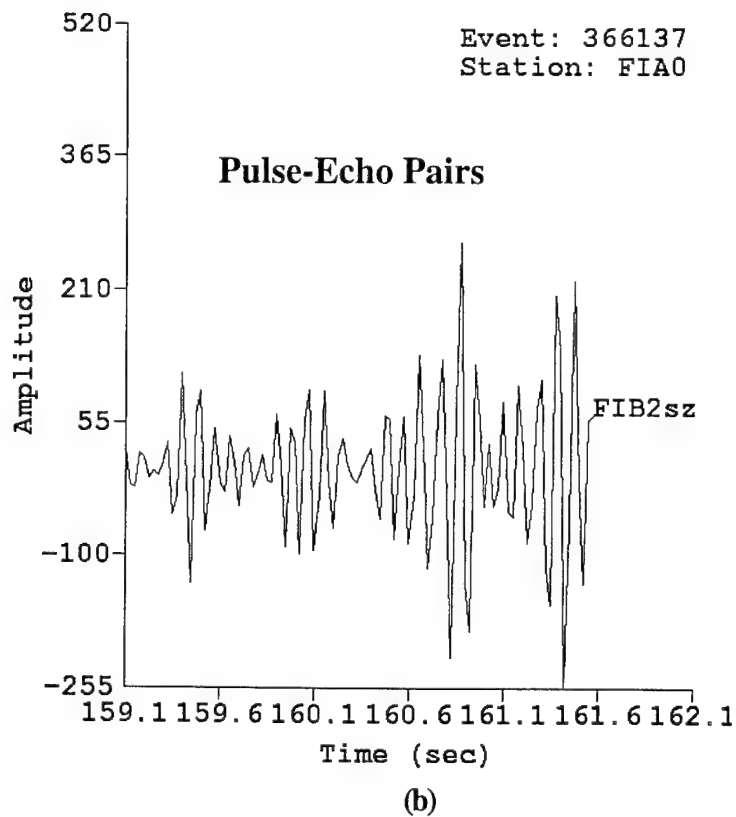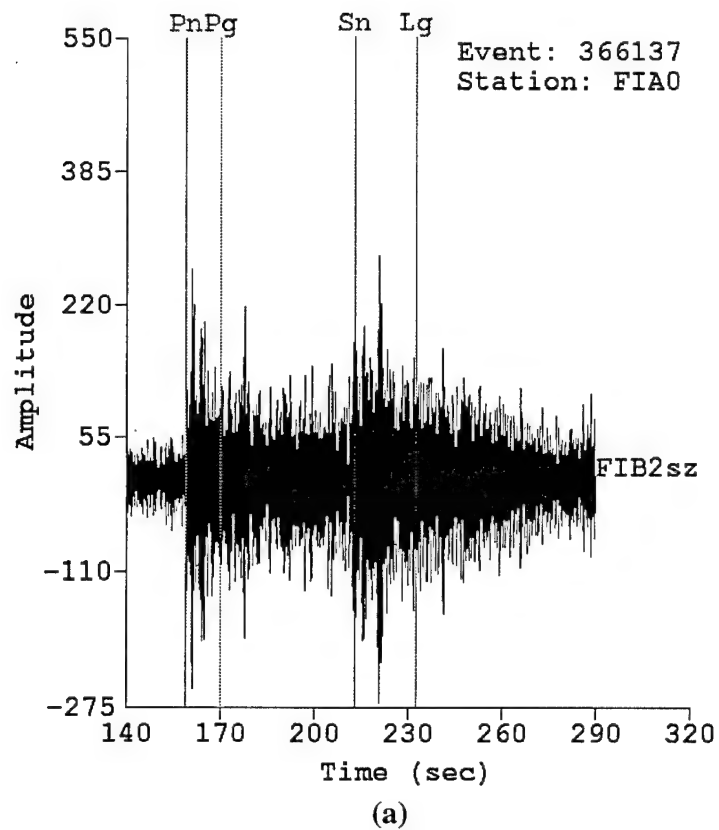
Figure 3: (a) Waveform for FINESA recording of a presumed blast in Region 1. (b) Expanded plot of the Pn coda showing periodic pulse-echo pairs.

8

will show that this pulse-echo pattern persists throughout the entire time series and is caused by the bubble pulse produced by the underwater explosion.

Figure 4 compares incoherent beam waveform envelopes for the Region 1 event recorded at the two arrays, FINESA (a) and NORESS (b). These envelopes were computed from 1 second time windows averaged across all the vertical component traces of the arrays after the traces were bandpass filtered in 9 frequency bands. The waveform envelopes recorded at these two arrays differ in the relative amplitudes of the phases and the fact that the Pn and Sn phases are much less apparent at NORESS than at FINESA. Since this is the same event, the difference in waveform envelope shapes must be due to differences in the propagation paths and the difference in the distances. Perhaps the Sn phase is attenuated along its path from Region 1 to NORESS, although the Pg and Lg waves seem to propagate efficiently along this path.

Figure 5 (a) and (b) show array-averaged spectra computed for the events in Figure 4. These spectra were computed for time windows on each of the phases beginning at the start times shown in Figure 4 and on the noise ahead of the Pn phase. Spectra were computed on all the traces of the arrays and averaged and the NORESS short-period instrument response was removed. These plots show a very clear spectral modulation or scalloping which is the same in all the phase spectra. This scalloping is obviously not apparent in the noise. This scalloping results from the interference and correlation of the pulse-echo pairs which comprise the entire waveform.

Figure 6 (a) and (b) show the cepstra computed from the spectra in Figure 5 (a) and (b), using methods described by Baumgardt and Ziegler (1988) and Baumgardt et al (1991a). In brief, the linear trends of the spectrums in Figure 6 were removed and low-frequency blowup, due the removal of the instrument response, was removed. The logarithm of the instrument corrected amplitude spectrum was then Fourier transformed to produce the cepstrums in Figure 6.

Time independent spectral modulations should produce cepstral peaks which line up in quefrency for all associated phases. The MERSY system in ISEIS automatically identifies such phases. The vertical line in Figure 6 (a) and (b) marks the cepstral peaks so identified by MERSY which have the same quefrency at both the FINESA and NORESS arrays. The main cepstral peaks line up at quefrencies of about 0.45 seconds, or 450 milliseconds. This cepstral peak is very strong at both arrays and indicates that the seismograms at both arrays consist of a series of pulse-echoes with time delays of 450 ms.

9
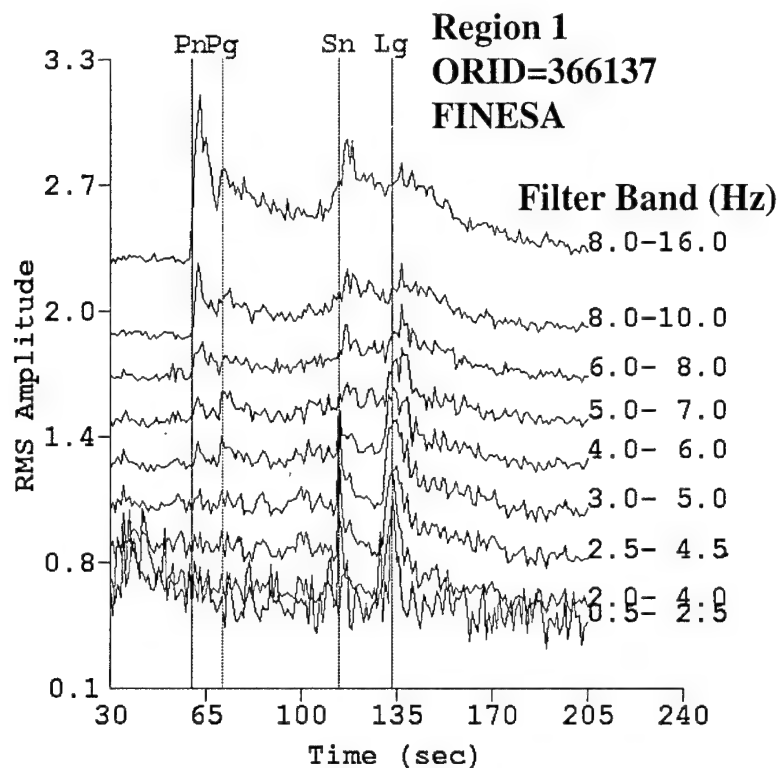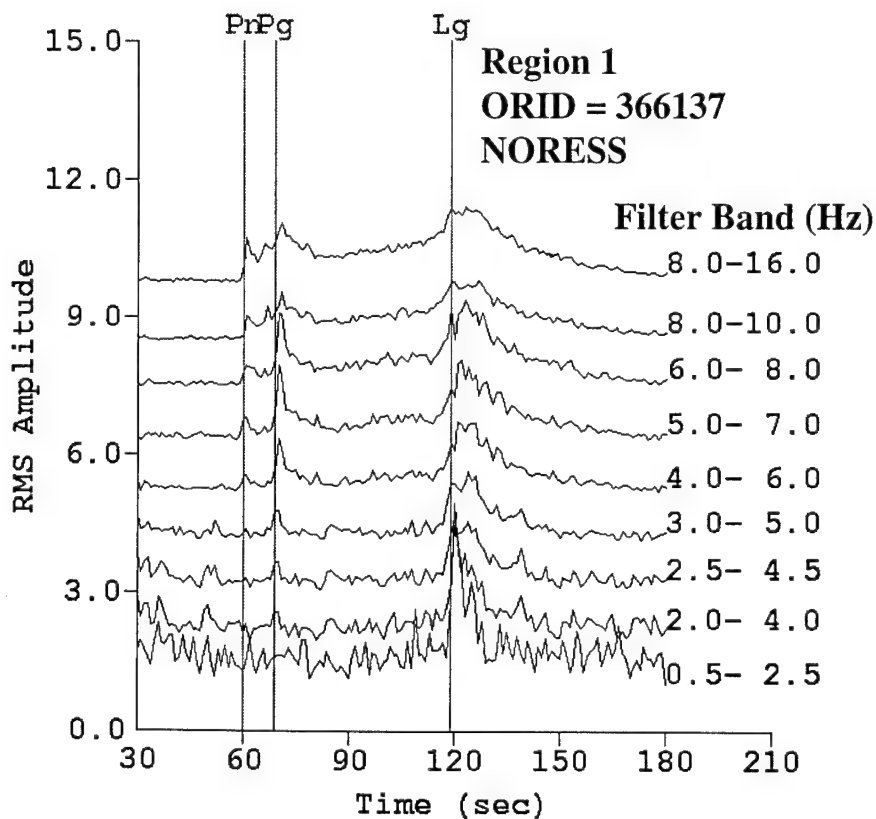
Figure 4: (a) Incoherent beam plots for waveform in Figure 3(a) recorded at FINESA. (b) Incoherent beam for the same event recorded at NORESS. The waveforms were prefiltered in the 9 filter bands indicated. Beams have been shifted for display.
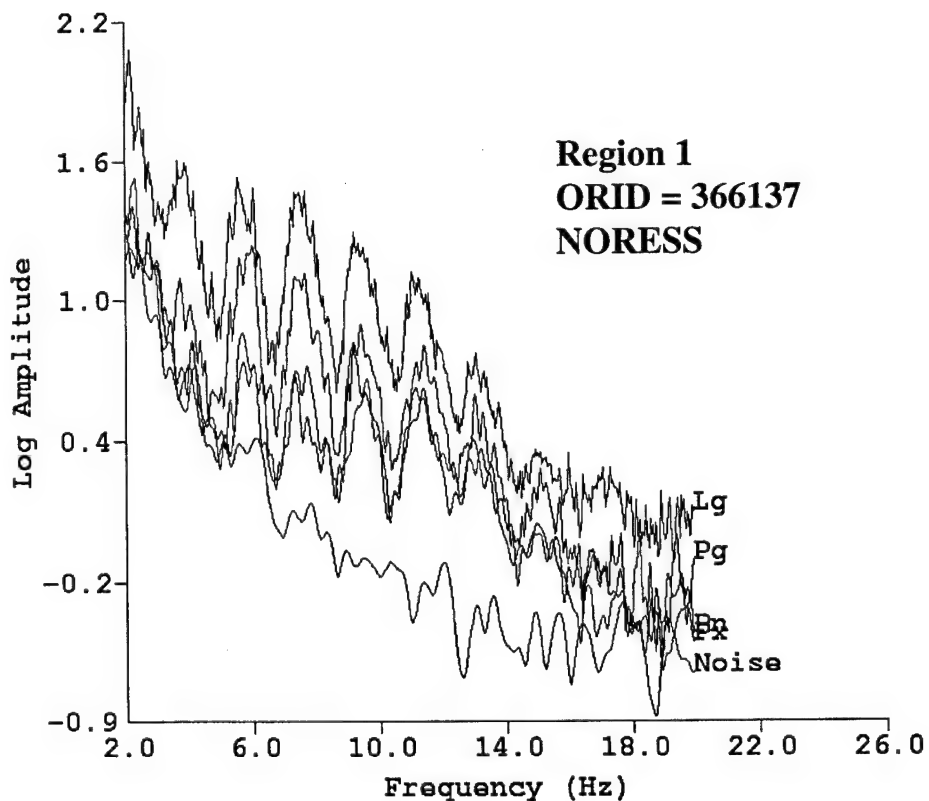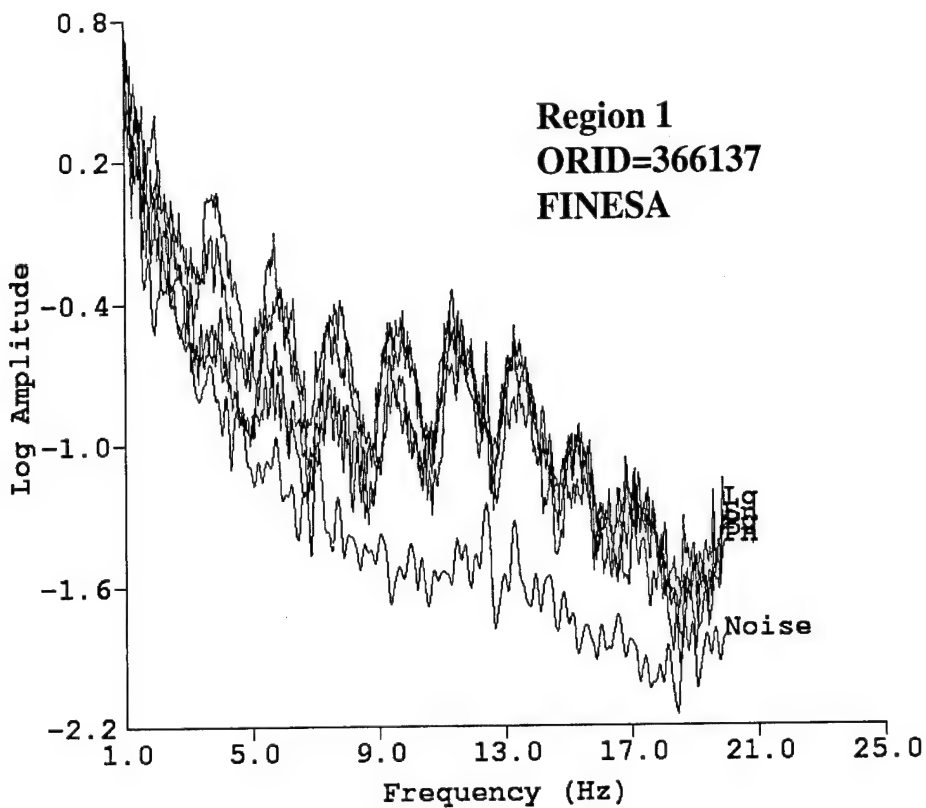
Figure 5: (a) Array-averaged signal and noise spectra for the Region 1 event shown in Figure 4(a) recorded at FINESA. (b) Array-averaged signal and noise spectra for the event shown in Figure 4(b) recorded at NORESS. Spectra have been corrected for instrument.

11
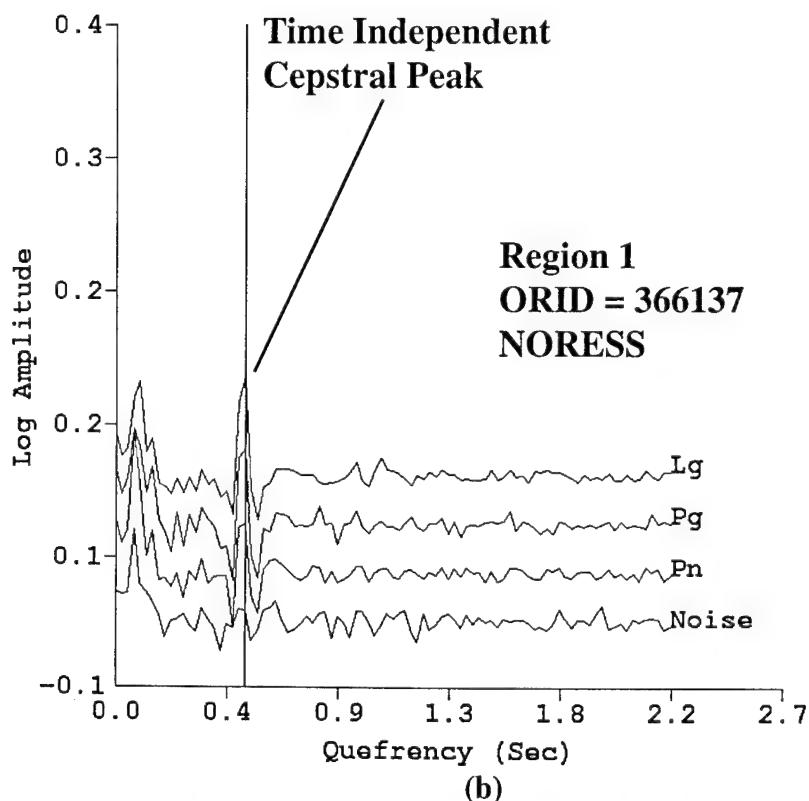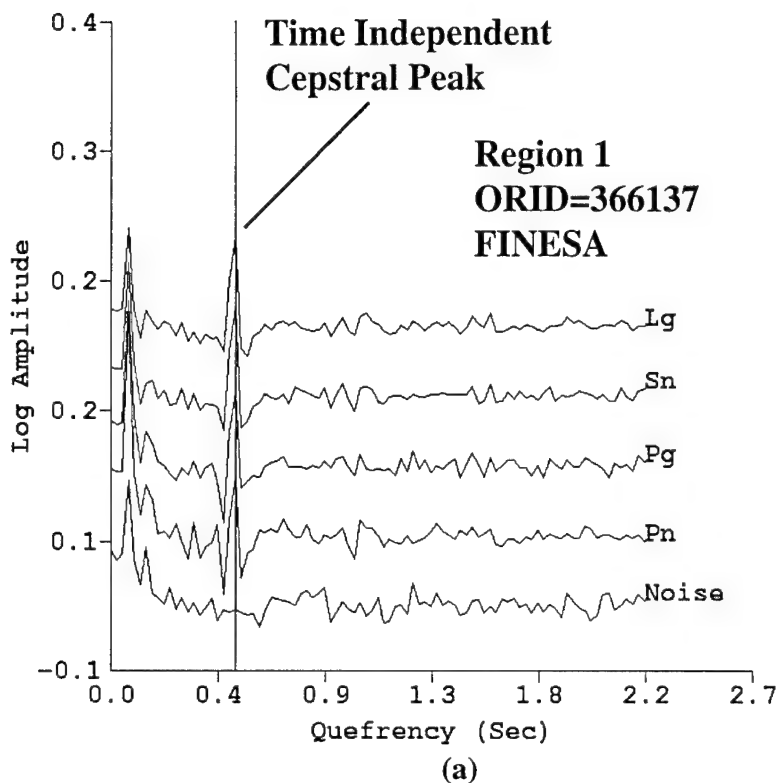
Figure 6: (a) Signal and noise cepstra computed from the spectra shown in Figure 3(a). (b) Signal and noise cepstra computed from the spectra shown in Figure 3(b). Time independent cepstral peaks corresponding to the pulse-echo pairs and picked by MERSY are shown. Phase cepstra are shifted up relative to the noise cepstra for display purposes.

12

Figures 7 (a) and (b) show two examples of the earlier offshore Stavenger events, recorded only at NORESS. As in the case of the Gulf of Bothnia event, these spectra have a very evident spectral scalloping which is the same in all the four phases associated with the event.

Figures 8 (a) and (b) show the cepstra computed for the two events. Both events have cepstral peaks at times less than 0.4 second. MERSY also picked a second peak near 0.4 seconds on the cepstrum in Figure 8 (b). This peak is probably also present in Figure 8 (a) but wasn't strong enough to be selected by the MERSY automatic peak picker.

Figure 9 (a) through (f) shows a selection of cepstra from several events. The peaks labeled **BP** are interpreted as resulting from the interference of the primary and bubble-pulse signals generated by the explosions. Generally, these events seem to have delay times between 0.4 and 0.65 seconds.

We also have observed peaks at lower quefrency for some of the events. Figure 9 (c) and (e) shows examples of one such peak at about 0.2 to 0.25 seconds which was recorded at both the NORESS and FINESA arrays at the same time. Figure 9 (f) is for event 70 in Region 2 in the middle of the Gulf of Bothnia. These peaks are labeled **WCB** which stands for "water column bounce" because the delay times are close to the expected two-way acoustic travel times in the water column. These peaks are sometimes associated with a negative peak (trough) at about 0.2 seconds or less, which MERSY usually doesn't pick up. MERSY only picks positive peaks. The low quefrency peaks observed for the southern Norway events in Figure 8 (a) and (b) may be other examples.

BUBBLE PULSE PERIODS

As mentioned above, these strong modulations observed in the spectra and the strong cepstral peaks in the cepstra of these events appear to result from the interference of the primary shock and bubble pulse in the water. Such phenomena have often been observed in offshore recordings on hydrophones. The strength of these signals recorded on land by seismic sensors attests to the efficient coupling of the explosions detonated in the water.

The dynamics of bubble pulses, or "cavitation," have been studied extensively in hydroacoustics since World War II. Figure 10 schematically illustrates how bubble pulses
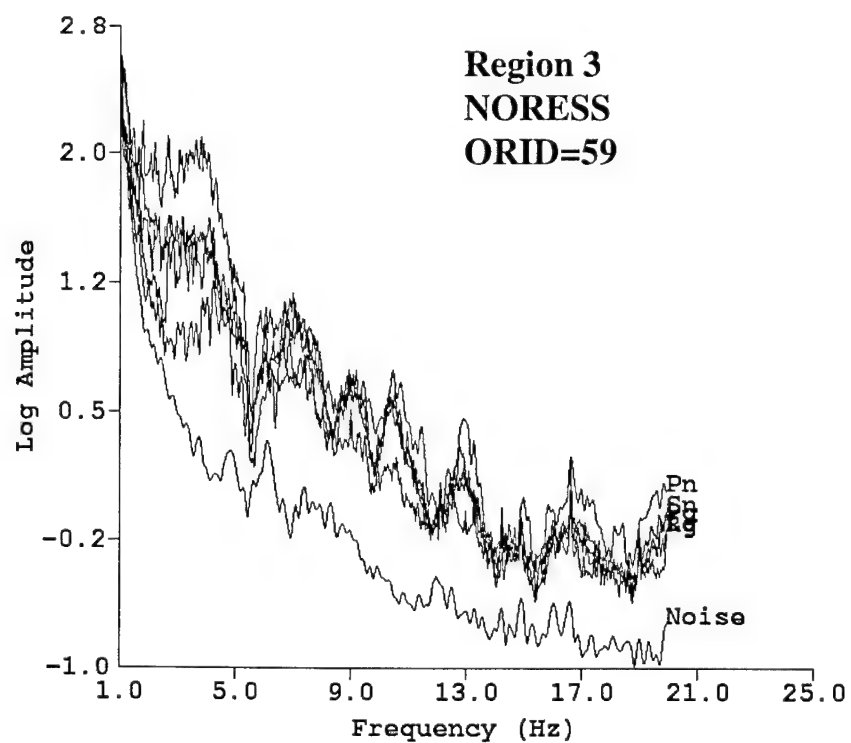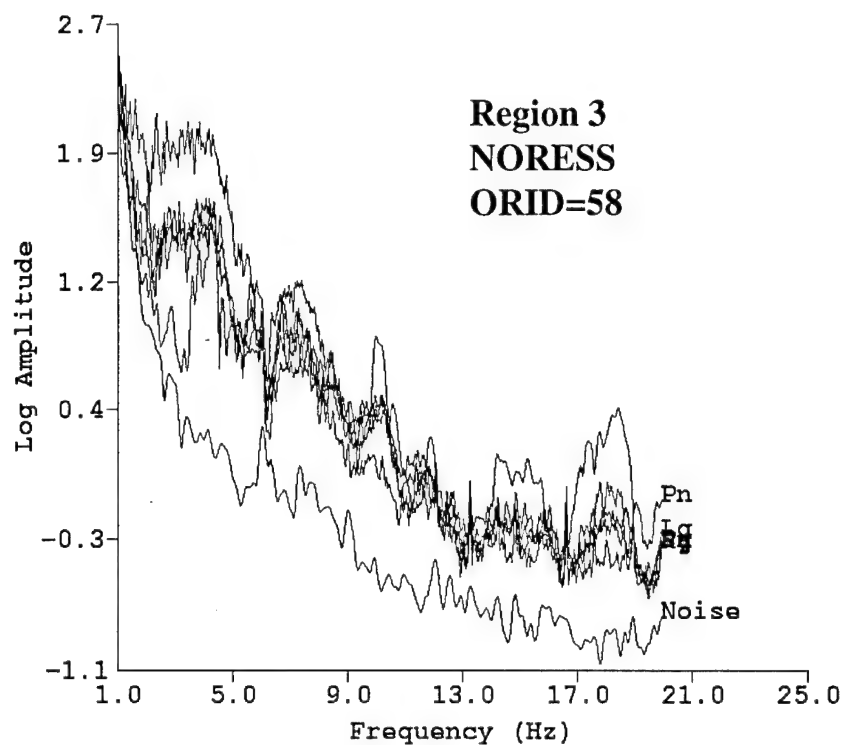
Figure 7: (a,b) Signal and noise array-averaged NORESS spectra for two of the sequence of events which occurred in the Baltic Sea south of the Stavenger region of Norway. All spectra have been corrected for instrument response.

14
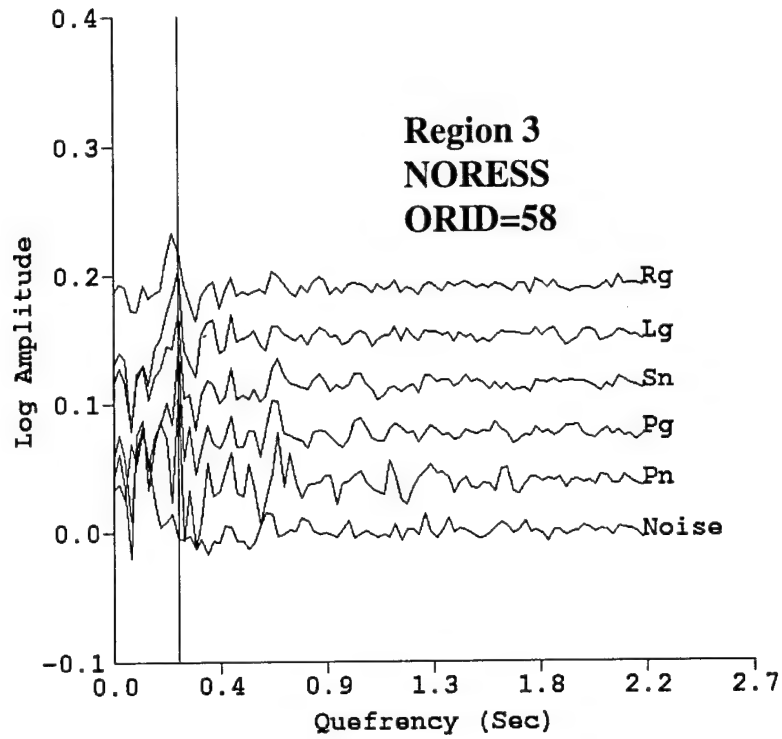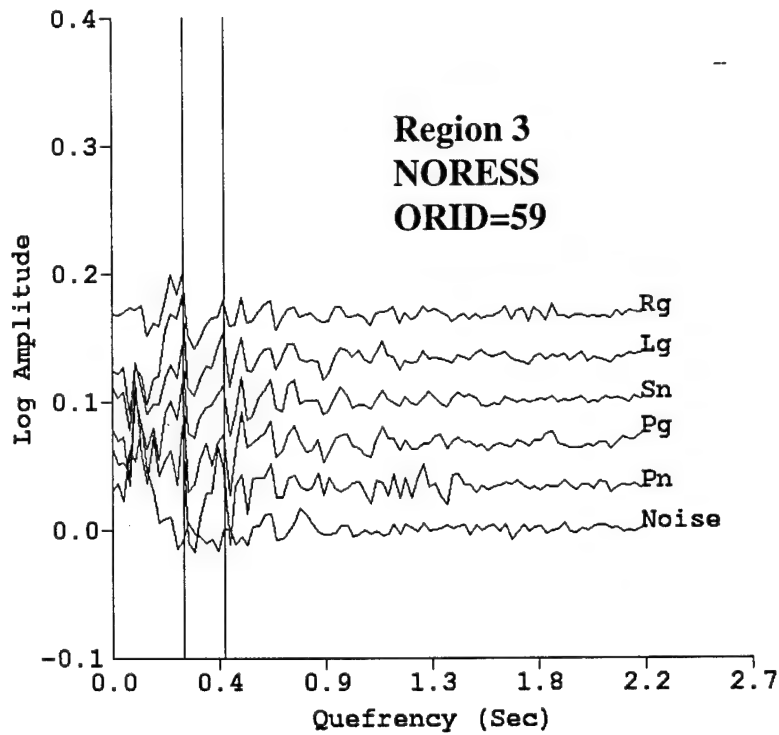
Figure 8: (a,b) Cepstra corresponding to the spectra shown in Figure 7 for the Region 3 events recorded at NORESS. Time independent cepstral peaks indicate the delay time for the pulse-echo signals that produce the spectral modulations in Figure 7. Phase cepstra are shifted up relative to the noise cepstra for display purposes.

15
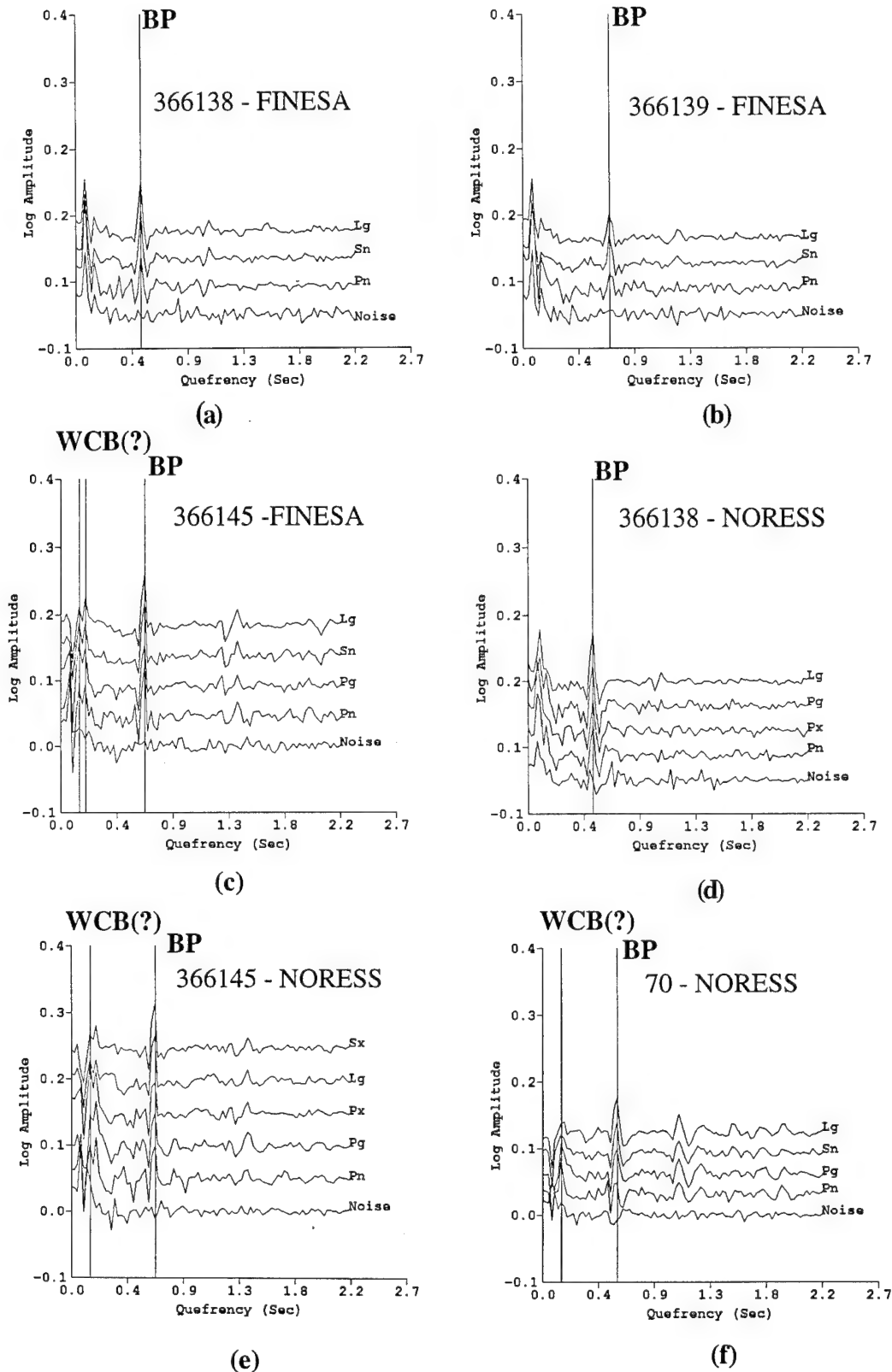
Figure 9: Cepstra of various events showing time independent cepstral peaks due to pulse-echos pairs. (a) Region 1 - FINESA. (b) Region 1 - FINESA. (c) Region 1 - FINESA. (d) Region 1 - NORESS. (e) Region 1 - NORESS. (f) Region 2 - NORESS. Bubble pulse (BP) peaks and water column reflection (WCB) peaks are indicated. All phase cepstra have been shifted up from the noise cepstra for viewing purposes.

16
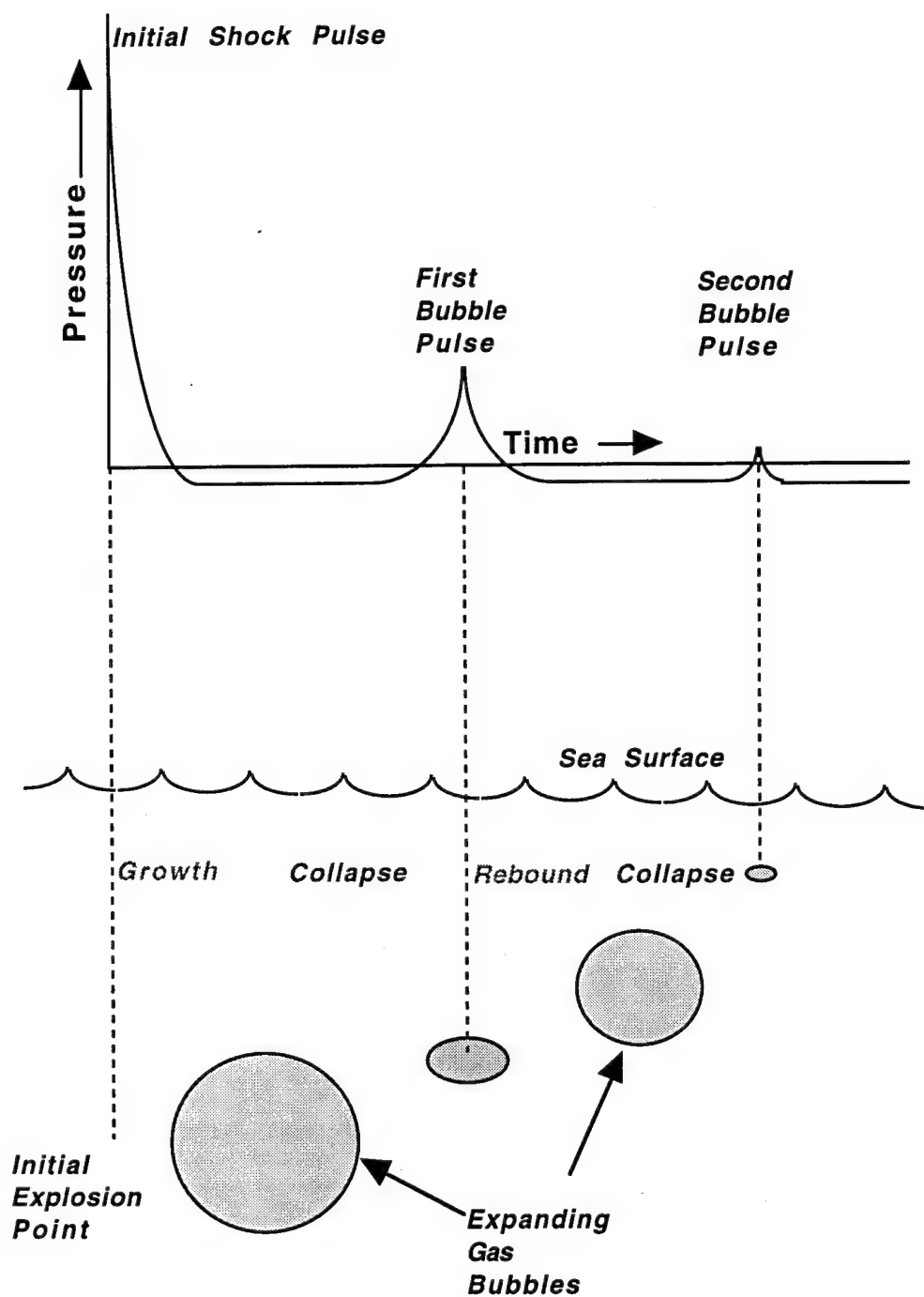
Figure 10: Schematic illustration showing how pressure pulses are produced by pulsations and migration of the bubble pulse. Positive pressure pulses are produced by the compression and rebound of the gas spheres generated by the underwater explosion. (After Urick, 1983).

from underwater explosions produce pressure pulses recorded acoustically and seismically. After the initial shock front is produced by the explosion, there follow a series of positive pressure pulses generated by the expanding and contracting gas sphere which rises to the surface. The amplitude of the pulses decays steadily as the energy in the expanding gas spheres dissipates and as the bubble rises to the surface.

As shown in Figure 10, the pressure can be negative during the last stage of the growth of the bubble and the initial phase of collapse (Ross, 1976). The acoustic signals in the water are produced by the bubble during the rebound phase, and the pressure pulse is positive. Theoretically, for explosions which produce vaporous bubbles, the positive pressure pulse will be higher frequency than the negative pressure pulse and much larger in amplitude. If the partial gas pressure in the bubble is less than 2% of the peak pressure in the bubble at maximum radius in the growth stage, the amplitude of the positive pulse will exceed the negative pulse amplitude by a factor of several hundred (Ross, 1976, p. 220). Measurements indicate that the second bubble pulse amplitude will decay to 1/5 the amplitude of the first bubble pulse (Urick, 1983).

Thus, for smaller underwater blasts, we would expect to only observe one of the bubble pulses, and it would have the same polarity as the primary pressure pulse. The acoustic pressure time function would be

$$p(t)=p_e(t)+p_b(t-T).$$ (1)

where p_e is the explosion pressure function, p_b is the bubble pulse pressure function, and T is the delay time between the initial explosion time the first rebound phase for the first bubble pulse. We assume the second bubble pulse pressure falls below the recording threshold of the acoustic/seismic sensor. Assuming perfect correlation, except for amplitude, between the explosion and bubble pulse, we have

$$p(t)=p_e(t)+\alpha p_e(t-T),$$ (2)

where α is the amplitude scaling constant, which is between 0 and 1. The power spectrum, $P(\omega)$ of (2), is then

$$P(\omega)=P_e(\omega)(1+\alpha^2+2\alpha\cos\omega T),$$ (3)

where P_e is the power spectrum of the initial pressure pulse. Thus, (3) shows that the single bubble-pulse model will produce a spectrum consisting of the spectrum of the initial explosion pressure function modulated by a periodic function with frequency periodicity of the inverse of the bubble-pulse time delay.

The time delay between the explosion pressure pulse and the first bubble pulse has been derived from theory (Willis, 1941) and verified by a number of studies (Cole, 1948) to be of the form

$$T = \frac{Kw^{1/3}}{(d+33)^{5/6}},\tag{4}$$

where K is a proportionality constant, which depends on the type of explosive, w is the charge size in lbs, and d is the depth of the explosions in ft. For TNT, K is equal to 4.4.

Figure 11 shows plots of the bubble pulse delay time versus water depth for charge sizes ranging from 10 to 2000 lbs. We do not know the exact yields of these charges, but the delay times and depths of the events in the Gulf of Bothnia and in the Baltic Sea are consistent with charge yields on the order of 10 to over 100 lbs.

WATER COLUMN REVERBERATIONS

As we pointed out above, a number of cepstra had low quefrency peaks. Figures 8 (a) and (b) show some examples for the Baltic Sea region. The event in Figure 8 (a) has a peak near 250 ms which was picked by MERSY. This same peak is also evident in Figure 8 (b) as well as the higher quefrency peak at about 400 ms, both of which were automatically picked by MERSY. It should be noted that MERSY only picks positive peaks. The low quefrency peaks may actually be negative, such as those shown in Figures 9 (c), (e), and (f). Negative cepstral peaks correspond to a multiple source where the second pulse has reversed polarity relative to the first pulse. Thus, these low-quefrency peaks may result from a single water-column reverberation (WCB), which would be expected to have reversed polarity relative to the initial explosion shock pulse.

The water depths in the Gulf of Bothnia are, on average, about 388 ft. Assuming sound speed of 5000 ft/sec, this gives an approximate delay time (two way travel time) of about 155 ms. This is consistent with the time delays observed in Figure 9 for the Gulf of Bothnia. For the Baltic Sea, the water depths are on average about 984 ft which gives

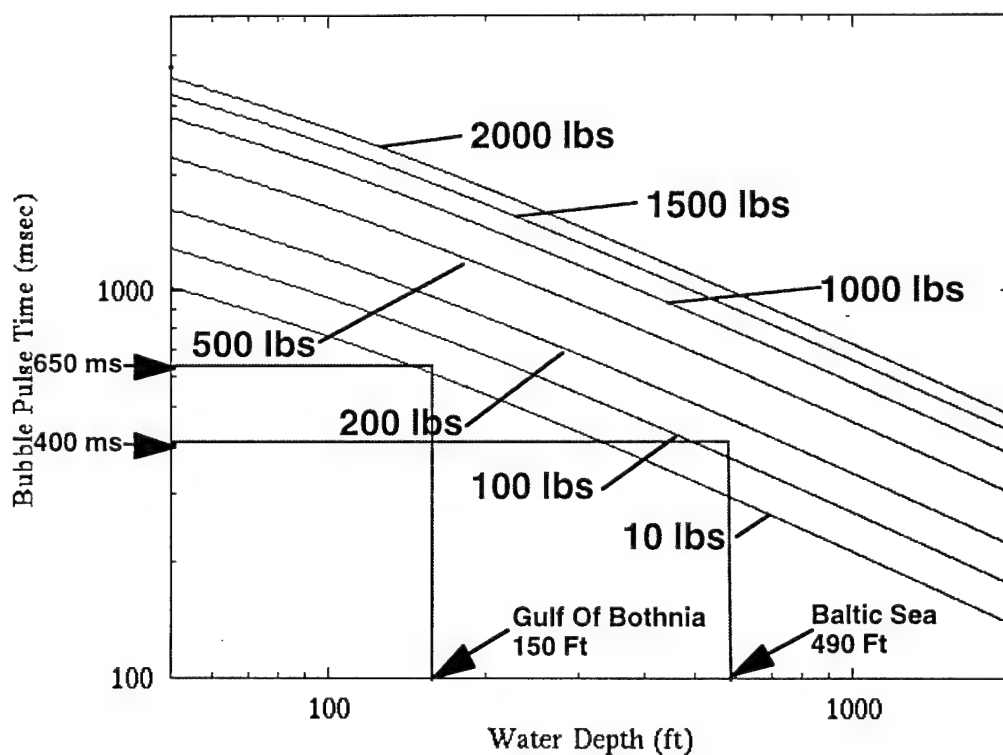# Bubble Pulse Period Versus Water Depth for Different Charge Sizes

Figure 11: Curves of theoretical bubble-pulse delay times versus water depth of charge for different charge sizes. The average water depths and observed delay times for charges in the Gulf of Bothnia and Baltic Sea are shown in red, which give yields of charges between 10 lbs for the Gulf of Bothnia to greater than 100 lbs for the Baltic Sea.

longer delays of about 393 ms. Again, this delay is consistent with those observed for the Baltic Sea in Figure 8.

REGIONAL *P/S* AMPLITUDE RATIOS

Recent discrimination studies have shown that the high-frequency ratio between the amplitude of the regional P (*Pn, Pg*) and S (*Sn, Lg*) can discriminate explosions and earthquakes. For example, Baumgardt and Young (1990) showed that in Scandinavia, explosions have higher *Pn/Sn* and *Pn/Lg* ratios than earthquakes in the 8-10 Hz band. We now consider the presumed underwater explosions to see if they have ratios expected for explosions.

Figure 12 compares frequency filtered NORESS waveforms for one of the Baltic Sea events (ORID = 58) (a) and a nearby event (ORID = 192482) (b) which is known to be an earthquake because it was felt in the region (NORSAR Staff, personal communication). The major identified phases, *Pn*, *Pg*, *Sn*, and *Lg* are indicated. Comparing these two events shows clearly that the shear waves are small for the explosion in Figure 12 (a) at frequencies above 8 Hz but remain large for the earthquake in Figure 12 (b). So, the discriminant seems to hold in this case.

Figure 13 (a) and (b) shows two events, both presumed blasts, recorded at NORESS from the Gulf of Bothnia. These examples present a very different picture than the Baltic Sea blast in Figure 12 (a). In these cases, the shear waves remain large at high frequency. Large *Pg* waves are evident in the 3-5 and 4-6 Hz bands for the event (ORID=366145), but otherwise, the *Pn* waves are very emergent in all frequency bands. The *Lg* energy seems to exceed the *Pn* energy in all bands.

In Figure 14, the measurements of the logarithm of the *Pn/Lg* amplitude ratio in the 8 to 10 Hz band are shown plotted versus distance of the event from the stations. The ratios were computed using maximum rms amplitudes measured on the incoherent beams like those shown in Figure 4. All the data points shown, with the exception of the Gulf of Bothnia explosions, were measured at NORESS only. Some of the earthquake and mine blast points were taken from the study of Baumgardt and Young (1990). The more distant earthquake points between 780 and 900 km are measurements from the Steigen earthquake swarm in Northern Norway recorded at the NORESS array (Atakan, 1992). The Gulf of Bothnia points at about 540 km are the measurements at FINESA for the 1992 events.

21
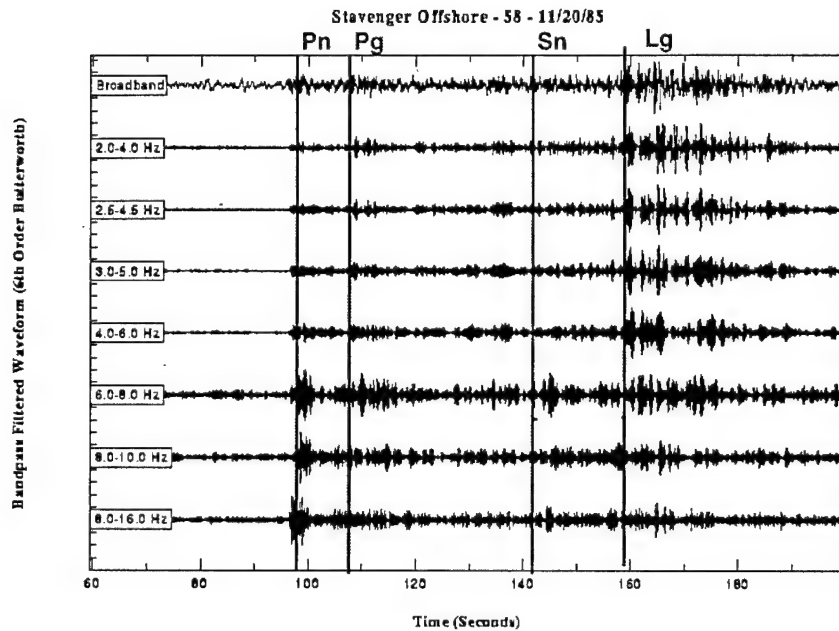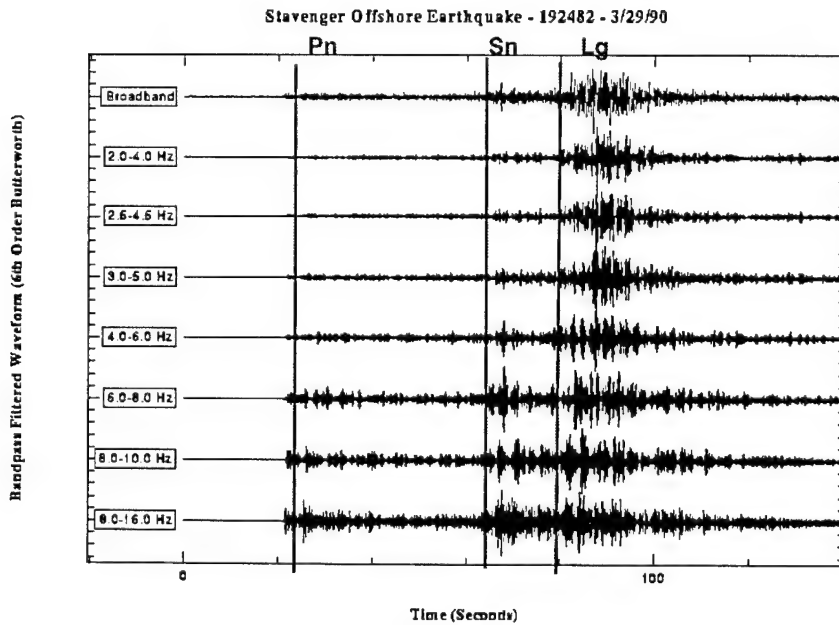
Figure 12: (a) Broadband and filtered NORESS waveforms for one of the Stavenger offshore presumed underwater blasts in Region 3. (b) NORESS waveforms for an earthquake in the same region which was "felt." Comparison of (a) with (b) shows that the explosion has larger *Pn* than *Sn* and *Lg* at high frequency whereas the earthquake has larger *Sn* and *Lg* than *Pn*.

22
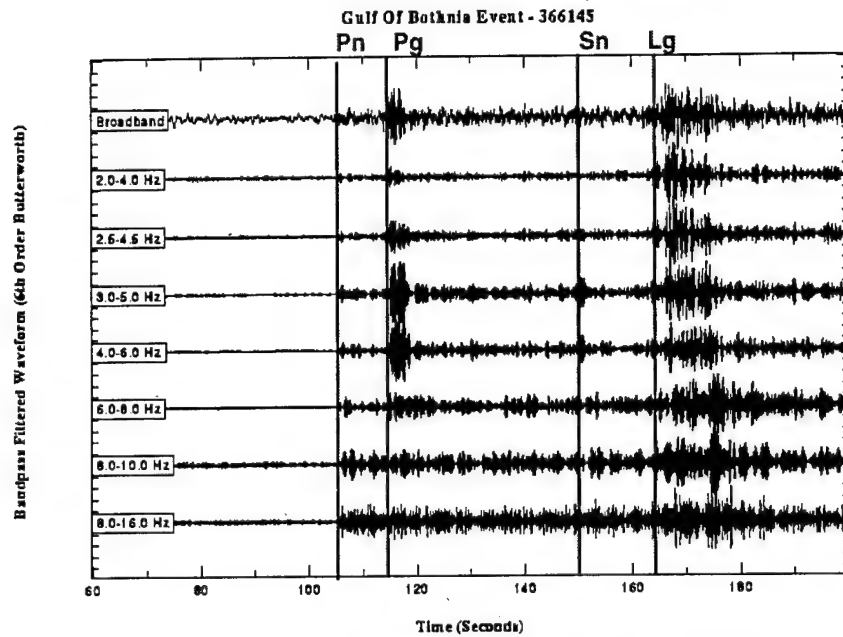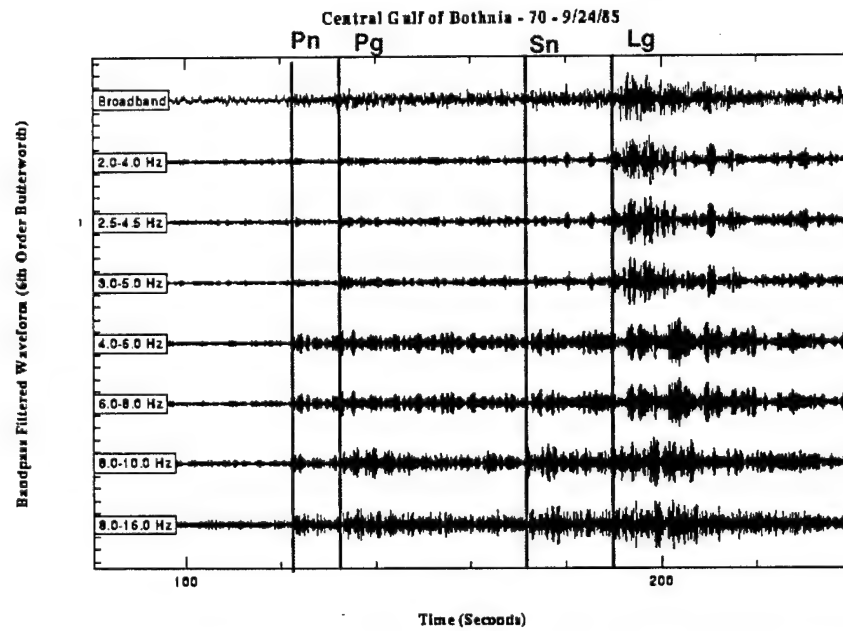
Figure 13: Comparison of broadband and filtered NORESS waveforms for two events in the Gulf of Bothnia, one in Region 1 (a) and the Region 2 (b) events. These plots show that at high frequency the *Sn* and *Lg* waves are less amplitude than the *Pn* waves.

8.0 - 10.0 Hz

□ : Earthquake
⊙ : Quarry Blast
△ : Marine Explosion
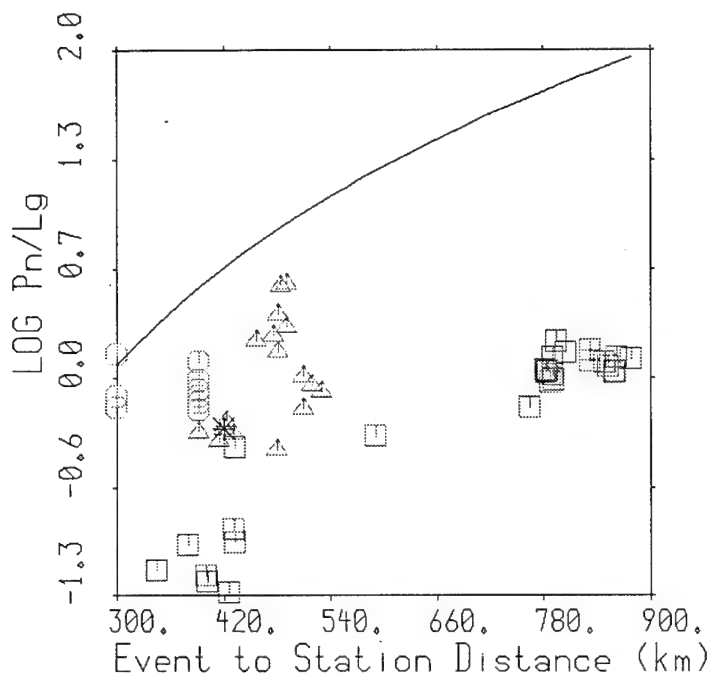
(a)
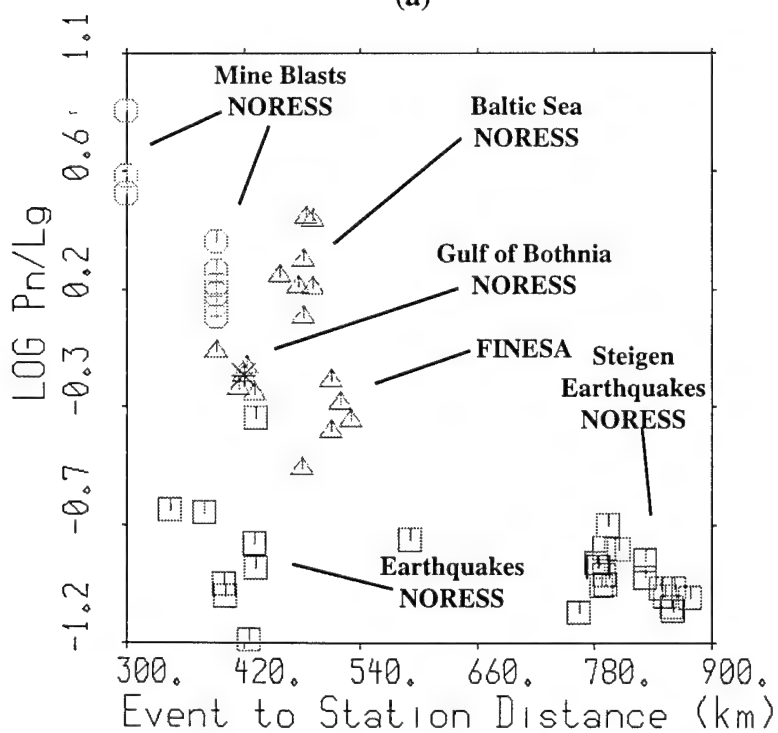
(b)

Figure 14: (a) Scatter plots as a function of distance of the *Pn/Lg* ratios for the under-water explosions and nearby earthquakes and explosion. Curve is the Sereno (1990) predicted distance dependence. (b) Same scatter plot corrected for distance using the Sereno (1990) curve.

24

The points in Figure 14 (a) are the raw data points uncorrected for distance. Also shown on this plot is a distance correction curve obtained by Baumgardt and Der (1995) from the single-phase amplitude versus distance formulas of Sereno (1990). Although this curve is above most of points, its shape seems to describe the distance dependence of the points. In Figure 14 (b), the ratios have been corrected to a common distance (500 km) using the curve.

This plot shows that the Baltic Sea events are clearly explosion like since they have *Pn/Lg* ratios comparable to the nearby Titania mine blasts and are above the earthquake points. However, the Gulf of Bothnia points are more enigmatic. They are lower than the Baltic Sea events and mine blasts and are comparable to the earthquakes, as is apparent in Figure 13. The Gulf of Bothnia events appear to have larger shear waves than what would be expected for most explosions.

What causes the large shear waves in the Gulf of Bothnia events? Mine blasts with large shear waves have been observed previously (Baumgardt, 1994). However, we usually associate these shear waves with rock fracturing or spalling in the mines. No such deformation occurs in underwater blasts. Assuming these events are blasts detonated in the water, shear waves cannot be produced by the source itself. The shear waves can only be coming from mode conversion from *P* waves in the sedimentary layers on the sea bottom and other discontinuities deeper in the crust.

Sereno and Orcutt (1987) have shown theoretically how oceanic phases, sometimes referred to as *Po* and *So* (Walker, 1982), can propagate efficiently in the oceanic lithosphere. Scattering may account for the large shear waves coming from the Gulf of Bothnia. Moreover, many studies have suggested that the attenuation of *Pn* may be greater than that of *Sn* in some ocean basins. Sereno and Orcutt (1987) have shown that the greater efficiency of *Sn* propagation is an intrinsic characteristic of the oceanic lithosphere. We observe weak *Sn* waves at NORESS as is evident in Figure 4. Perhaps the *Sn* energy has been scattered into *Lg* waves by heterogeneities along the path from the Gulf of Bothnia to NORESS. These same characteristics may exist for the paths from the Gulf of Bothnia to NORESS and FINESA. The larger *Pn/Lg* ratio for the Baltic Sea-to-NORESS path may be due to low *P*-to-*S* scattering there. The sediment properties in the Baltic Sea may be different than those in the Gulf of Bothnia, which may account for the different scattering levels.

CONCLUSIONS

This study has shown the efficiency of coupling of acoustic sources in the water to seismic sensors well inland which means that near-coast underwater blasting activities can be monitored seismically. Thus, hydroacoustic sensors and extreme high-frequencies are not required to monitor possible blasting activity in shallow marine environments. The seismic methods developed for monitoring ripple firing in mine blasts can also be exploited for the detection of bubble pulses in underwater blasts.

Underwater explosions are somewhat analogous to decoupled explosions in large cavities because the seismic wave generation is almost entirely elastic: no inelastic deformations are involved. Of course, the coupling in water is much better than gas coupling in a large cavity in rock. However, even though the underwater blast sources are purely compressional, large shear waves can be generated. This again indicates that caution must be used when using the *P/S* ratio discriminant, as pointed out by Baumgardt (1994). The sediment conditions in the Gulf of Bothnia seem to be ideal for the generation of large shear waves and an underwater blast can be made to look like an earthquake. In such cases, the bubble pulse must be detected to identify the event as an explosion.

This then raises the question of whether an evasion scenario can be devised to make the explosion in the ocean look like an earthquake and destroy the bubble pulse. One possibility, similar to the scenario suggested by White et al (1994), would be a detonation in the shallow ocean where the bubble would break the surface before the collapse pulse is produced. Thus, the explosion may be enough contained to not be picked up atmospherically but the bubble pulse would not be observed acoustically or seismically. However, the primary and single-water column reverberation could be picked up and the explosion may identified. Thus, when monitoring underwater explosions, no one single discriminant can be relied upon by itself, and all possible evasion scenarios need to be considered.

REFERENCES

Atakan, K. (1992). An unusual earthquake sequence in Steigen Northern Norway, Internal Report, Institute of Solid Earth Physics, University of Bergen, Norway.

BABEL Working Group (1993). Deep seismic reflection/refraction interpretation of crustal structure along BABEL profiles A and B in the southern Baltic Sea, *Geophys. J. Int.*, **112**, 325-343.

Bache, T.C., S.R. Bratt, J. Wang, R.M. Fung, C. Kobryn, and J.W. Given (1990). The Intelligent Monitoring System, *Bull. Seism. Soc. Am.*, **80**, 2261-2281.

Baumgardt, D.R. (1994). The Kiruna mine blasts of Northern Sweden: Case study of the failure of the *P/S* ratio discriminant, Topical Report, August 31, 1994.

Baumgardt, D.R. and K.A. Ziegler (1988). Spectral evidence of source multiplicity in explosions: application to regional discrimination of earthquakes and explosions, *Bull. Seism. Soc. Am.*, **78**, 1773-1795.

Baumgardt, D.R. and G. Young (1990). Regional seismic waveform discriminants and case based event identification using regional arrays, *Bull. Seism. Soc. Am.*, **80**, Part B, 1874-1892.

Baumgardt, D.R., G.B. Young, and K.A. Ziegler (1991a). Design and Development of the Intelligent Event Identification System: Design Considerations and Processing for Regional Event Identification, *Scientific Report No. 1*, PL-TR-91-2211, 29 August 1991, ENSCO, Inc., ADA246793

Baumgardt, D.R., S. Carter, M. Maxson, J. Carney, K. Ziegler, and N. Matson (1991b). Design and development of the intelligent event identification system, *PL-TR-91- 2298(I)*, Final Report, ENSCO, Inc., Springfield, VA, ADA248381.

Cole, R.H. (1948). *Underwater Explosions*, Princeton University Press, Princeton, N.J.

Mitchell, S.K. and N.R. Bedford (1976). Determination of source depth from the spectra of small explosions observed at long ranges, *J.Acoust. Soc. Am.*, **60**, 825-828.

Phillips, D.W. (1995). Hydroacoustic monitoring technologies, in *Proceedings, CTBT Monitoring Technologies Conference*, H1-1 - H1-2, Carmel Highland Doubletree, San Diego, CA, 26-29 September 1994.

Ross, D. (1976). *Mechanics of Underwater Noise*, Pergamon Press, New York.

Sereno, T.J. (1990). Simulation of the detection and location capability of regional seismic networks in the Soviet Union, Final Report, SAIC-91/1061, SAIC, San Diego, CA.

Sereno, T.J. and J.A. Orcutt (1987). Synthetic *Pn* and *Sn* phases and the frequency dependence of *Q* of the oceanic lithosphere, *J. Geophys. Res.*, **92**, 3541-3566.

Suteau-Henson, A. and T.C. Bache (1988). Spectral characteristics of regional phases recorded at NORESS, **78**, 708-725.

Urick, R.J. (1983). *Principals of Underwater Sound*, McGraw-Hill, Inc., New York.

Walker, D. (1982). Oceanic PN/SN phases: A qualitative explanation and reinterpretation of the *T*-phase, *Repl HIG-82-6*, 19p pp., Hawaii Inst. of Geophys., Honolulu.

White, J.W., M. Kamegai, and D.B. Clarke (1994). Scenario analysis of clandestine nuclear tests at sea, in *Proceedings, CTBT Monitoring Technologies Conference*, H4-1-H4-4, Carmel Highland Doubletree, San Diego, Ca., 26-29 September 1994.

Willis, H.F. (1941). Underwater explosions, time interval between successive explosions, British Report *WA-47-21*.

Prof. Thomas Ahrens
Seismological Lab, 252-21
Division of Geological & Planetary Sciences
California Institute of Technology
Pasadena, CA 91125

Prof. Keiiti Aki
Center for Earth Sciences
University of Southern California
University Park
Los Angeles, CA 90089-0741

Prof. Shelton Alexander
Geosciences Department
403 Deike Building
The Pennsylvania State University
University Park, PA 16802

Dr. Thomas C. Bache, Jr.
Science Applications Int'l Corp.
10260 Campus Point Drive
San Diego, CA 92121 (2 copies)

Prof. Muawia Barazangi
Cornell University
Institute for the Study of the Continent
3126 SNEE Hall
Ithaca, NY 14853

Dr. Douglas R. Baumgardt
ENSCO, Inc
5400 Port Royal Road
Springfield, VA 22151-2388

Dr. T.J. Bennett
S-CUBED
A Division of Maxwell Laboratories
11800 Sunrise Valley Drive, Suite 1212
Reston, VA 22091

Dr. Robert Blandford
AFTAC/TT, Center for Seismic Studies
1300 North 17th Street
Suite 1450
Arlington, VA 22209-2308

Dr. Steven Bratt
ARPA/NMRO
3701 North Fairfax Drive
Arlington, VA 22203-1714

Dale Breding
U.S. Department of Energy
Recipient, IS-20, GA-033
Office of Arms Control
Washington, DC 20585

Dr. Jerry Carter
Center for Seismic Studies
1300 North 17th Street
Suite 1450
Arlington, VA 22209-2308

Mr Robert Cockerham
Arms Control & Disarmament Agency
320 21st Street North West
Room 5741
Washington, DC 20451,

Dr. Zoltan Der
ENSCO, Inc.
5400 Port Royal Road
Springfield, VA 22151-2388

Dr. Stanley K. Dickinson
AFOSR/NM
110 Duncan Avenue
Suite B115
Bolling AFB, DC

Dr Petr Firbas
Institute of Physics of the Earth
Masaryk University Brno
Jecna 29a
612 46 Brno, Czech Republic

Dr. Mark D. Fisk
Mission Research Corporation
735 State Street
P.O. Drawer 719
Santa Barbara, CA 93102

Dr. Cliff Frolich
Institute of Geophysics
8701 North Mopac
Austin, TX 78759

Dr. Holly Given
IGPP, A-025
Scripps Institute of Oceanography
University of California, San Diego
La Jolla, CA 92093

Dr. Jeffrey W. Given
SAIC
10260 Campus Point Drive
San Diego, CA 92121

Dan N. Hagedon
Pacific Northwest Laboratories
Battelle Boulevard
Richland, WA 99352

Dr. James Hannon
Lawrence Livermore National Laboratory
P.O. Box 808, L-205
Livermore, CA 94550

Dr. Roger Hansen
University of Colorado, JSPC
Campus Box 583
Boulder, CO 80309

Prof. Danny Harvey
University of Colorado, JSPC
Campus Box 583
Boulder, CO 80309

Prof. Donald V. Helmberger
Division of Geological & Planetary Sciences
California Institute of Technology
Pasadena, CA 91125

Prof. Eugene Herrin
Geophysical Laboratory
Southern Methodist University
Dallas, TX 75275

Prof. Robert B. Herrmann
Department of Earth & Atmospheric Sciences
St. Louis University
St. Louis, MO 63156

Prof. Lane R. Johnson
Seismographic Station
University of California
Berkeley, CA 94720

Prof. Thomas H. Jordan
Department of Earth, Atmospheric &
  Planetary Sciences
Massachusetts Institute of Technology
Cambridge, MA 02139

Robert C. Kemerait
ENSCO, Inc.
445 Pineda Court
Melbourne, FL 32940

U.S. Dept of Energy
Max Koontz, NN-20, GA-033
Office of Research and Develop.
1000 Independence Avenue
Washington, DC 20585

Dr. Richard LaCoss
MIT Lincoln Laboratory, M-200B
P.O. Box 73
Lexington, MA 02173-0073

Prof. Charles A. Langston
Geosciences Department
403 Deike Building
The Pennsylvania State University
University Park, PA 16802

Jim Lawson, Chief Geophysicist
Oklahoma Geological Survey
Oklahoma Geophysical Observatory
P.O. Box 8
Leonard, OK 74043-0008

Prof. Thorne Lay
Institute of Tectonics
Earth Science Board
University of California, Santa Cruz
Santa Cruz, CA 95064

Dr. William Leith
U.S. Geological Survey
Mail Stop 928
Reston, VA 22092

Mr. James F. Lewkowicz
Phillips Laboratory/GPE
29 Randolph Road
Hanscom AFB, MA 01731-3010(2 copies)

Dr. Gary McCartor
Department of Physics
Southern Methodist University
Dallas, TX 75275

Prof. Thomas V. McEvilly
Seismographic Station
University of California
Berkeley, CA 94720

Dr. Keith L. McLaughlin
S-CUBED
A Division of Maxwell Laboratory
P.O. Box 1620
La Jolla, CA 92038-1620

Prof. Bernard Minster
IGPP, A-025
Scripps Institute of Oceanography
University of California, San Diego
La Jolla, CA 92093

2

Prof. Brian J. Mitchell
Department of Earth & Atmospheric Sciences
St. Louis University
St. Louis, MO 63156

Mr. Jack Murphy
S-CUBED
A Division of Maxwell Laboratory
11800 Sunrise Valley Drive, Suite 1212
Reston, VA 22091 (2 Copies)

Dr. Keith K. Nakanishi
Lawrence Livermore National Laboratory
L-025
P.O. Box 808
Livermore, CA 94550

Prof. John A. Orcutt
IGPP, A-025
Scripps Institute of Oceanography
University of California, San Diego
La Jolla, CA 92093

Dr. Howard Patton
Lawrence Livermore National Laboratory
L-025
P.O. Box 808
Livermore, CA 94550

Dr. Frank Pilotte
HQ AFTAC/TT
1030 South Highway A1A
Patrick AFB, FL 32925-3002

Dr. Jay J. Pulli
Radix Systems, Inc.
6 Taft Court
Rockville, MD 20850

Prof. Paul G. Richards
Lamont-Doherty Earth Observatory
 of Columbia University
Palisades, NY 10964

Mr. Wilmer Rivers
Multimax Inc.
1441 McCormick Drive
Landover, MD 20785

Dr. Alan S. Ryall, Jr.
Lawrence Livermore National Laboratory
L-025
P.O. Box 808
Livermore, CA 94550

Dr.Chandan K. Saikia
Woodward Clyde- Consultants
566 El Dorado Street
Pasadena, CA 91101

Mr. Dogan Seber
Cornell University
Inst. for the Study of the Continent
3130 SNEE Hall
Ithaca, NY 14853-1504

Secretary of the Air Force
(SAFRD)
Washington, DC 20330

Office of the Secretary of Defense
DDR&E
Washington, DC 20330

Thomas J. Sereno, Jr.
Science Application Int'l Corp.
10260 Campus Point Drive
San Diego, CA 92121

Dr. Michael Shore
Defense Nuclear Agency/SPSS
6801 Telegraph Road
Alexandria, VA 22310

Prof. David G. Simpson
IRIS, Inc.
1616 North Fort Myer Drive
Suite 1050
Arlington, VA 22209

Dr. Jeffrey Stevens
S-CUBED
A Division of Maxwell Laboratory
P.O. Box 1620
La Jolla, CA 92038-1620

Prof. Brian Stump
Los Alamos National Laboratory
EES-3
 Mail Stop C-335
Los Alamos, NM 87545

Prof. Tuncay Taymaz
Istanbul Technical University
Dept. of Geophysical Engineering
Mining Faculty
Maslak-80626, Istanbul Turkey

3

Prof. M. Nafi Toksoz
Earth Resources Lab
Massachusetts Institute of Technology
42 Carleton Street
Cambridge, MA 02142

Dr. Larry Turnbull
CIA-OSWR/NED
Washington, DC 20505

Dr. Karl Veith
EG&G
5211 Auth Road
Suite 240
Suitland, MD 20746

Prof. Terry C. Wallace
Department of Geosciences
Building #77
University of Arizona
Tuscon, AZ 85721

Dr. William Wortman
Mission Research Corporation
8560 Cinderbed Road
Suite 700
Newington, VA 22122

ARPA, OASB/Library
3701 North Fairfax Drive
Arlington, VA 22203-1714

HQ DNA
ATTN: Technical Library
Washington, DC 20305

Defense Technical Information Center
8725 John J. Kingman Road
Ft Belvoir, VA 22060-6218
                      2 copies

TACTEC
Battelle Memorial Institute
505 King Avenue
Columbus, OH 43201 (Final Report)

Phillips Laboratory
ATTN: GPE
29 Randolph Road
Hanscom AFB, MA 01731-3010

Phillips Laboratory
ATTN: TSML
5 Wright Street
Hanscom AFB, MA 01731-3004

Phillips Laboratory
ATTN: PL/SUL
3550 Aberdeen Ave SE
Kirtland, NM 87117-5776 (2 copies)

Dr. Michel Campillo
Observatoire de Grenoble
I.R.I.G.M.-B.P. 53
38041 Grenoble, FRANCE

Prof. Hans-Peter Harjes
Institute for Geophysic
Ruhr University/Bochum
P.O. Box 102148
4630 Bochum 1, GERMANY

Prof. Eystein Husebye
IFJF
Jordskjelvstasjonen
Allegaten 41, 5007 BERGEN NORWAY

David Jepsen
Acting Head, Nuclear Monitoring Section
Bureau of Mineral Resources
Geology and Geophysics
G.P.O. Box 378, Canberra, AUSTRALIA

Ms. Eva Johannisson
Senior Research Officer
FOA
S-172 90 Sundbyberg, SWEDEN

Dr. Peter Marshall
Procurement Executive
Ministry of Defense
Blacknest, Brimpton
Reading FG7-FRS, UNITED KINGDOM

Dr. Bernard Massinon, Dr. Pierre Mechler
Societe Radiomana
27 rue Claude Bernard
75005 Paris, FRANCE (2 Copies)

Dr. Svein Mykkeltveit
NTNT/NORSAR
P.O. Box 51
N-2007 Kjeller, NORWAY (3 Copies)

4

Dr. Jorg Schlittenhardt
Federal Institute for Geosciences & Nat'l Res.
Postfach 510153
D-30631 Hannover , GERMANY

Dr. Johannes Schweitzer
Institute of Geophysics
Ruhr University/Bochum
P.O. Box 1102148
4360 Bochum 1, GERMANY

Trust & Verify
VERTIC
Carrara House
20 Embankment Place
London WC2N 6NN, ENGLAND